EXPERIMENTAL STUDY ON SERPENTINIZATION OF IRON-RICH OLIVINE: IMPLICATIONS FOR MARS. Xi-Yu Wang[1,2], Yu-Yan Sara Zhao[1,3]*, Sen Hu[4], Hua-Pei Wang[5], Jun-Xiang Miao[5], Hong-Lei Lin[4,] Jun-Hu Wang[6], Chao Qi[4,2]*, Yang-Ting Lin[4], Shi-Ling Yang[4,2], Xiong-Yao Li[1,3], Jian-Zhong Liu[1,3]. [1]Center for Lunar and Planetary Sciences, Institute of Geochemistry Chinese Academy of Sciences, Guiyang, China. [2]College of Earth and Planetary Sciences, University of Chinese Academy of Sciences, Beijing, China. [3]CAS Center for Excellence in Comparative Planetology, Hefei, China. [4]Key Laboratory of Earth and Planetary Physics, Institute of Geology and Geophysics, Chinese Academy of Sciences, Beijing 100029, China., [5]Paleomagnetism and Planetary Magnetism Laboratory, School of Geophysics and Geomatics, China University of Geosciences, Wuhan 430074, China., [6]Center for Advanced Mössbauer Spectroscopy, Dalian Institute of Chemical Physics, Chinese Academy of Sciences, Dalian, China. (*Emails: zhaoyuyan@mail.gyig.ac.cn; qichao@mail.iggcas.ac.cn; xiyuwangxy@gmail.com)

Introduction: Serpentinization processes are essential for the geological and environmental evolution of a planetary body and important from an astrobiology perspective [1]. In particular, serpentinization indicates not only high-temperature and high-pressure processes but also hydrothermal environments [2]. On the Martian surface, basaltic crusts are widely distributed, but only a few serpentine exposures have been identified [3,4], such as Nili Fossae [1]. To aid in identifying signs of serpentinization processes on Mars and further constrain the history of water-rock interactions, detailed studies of serpentinization processes and resultant mineral assemblages are needed.

In terrestrial case studies and most experimental studies on serpentinization relevant to Mars, Mg-rich olivine (forsterite) is the primary focus [e.g.,5], mainly due to the lack of Fe-rich olivine on Earth. However, Fe-rich olivine (Fa# >20; Fe/(Fe+Mg)) is widely distributed on the Martian surface [6]. Fe olivine may lead to different reaction pathways during serpentinization. Fe redox is also the key to H_2 and methane (CH_4) production during serpentinization processes [5,7]. Previous experimental studies have explored factors influencing serpentinization processes, such as reaction temperature [5], reaction pressure [8], water flow velocity [9], olivine grain size [5], and initial basalt composition [10]. Here, we focus on the initial Fe contents in olivine and their role during serpentinization processes on Mars.

Methods: Fe-rich olivine samples (Fa100, Fa71, Fa50, and Fa29) were synthesized with details in ref. [11] for use in this study. Purchased pure forsterite (99% purity) from Alfa was also examined for comparison.

Since the grain size of olivine would substantially influence the reaction rates [5], we adapted a grain size <53 μm to ensure a complete reaction in a limited reaction time. We doped initial deoxygenated ultrapure water (dissolved O_2 < 1 ppm) with 50 wt% D_2O to facilitate tracing of the isotopic changes in H. The reaction temperature was set to 200°C, which is the critical *T* for H_2 start to be produced in the serpentinization system [5] and meets the working conditions of our experimental reactor. We set the reaction pressure to 15 MPa, and the pressure has been found to have no substantial influence on the final solid products of the reaction [8]. Each experiment ran for 20 days, and during the experiments, the whole system was under pure Ar gas conditions.

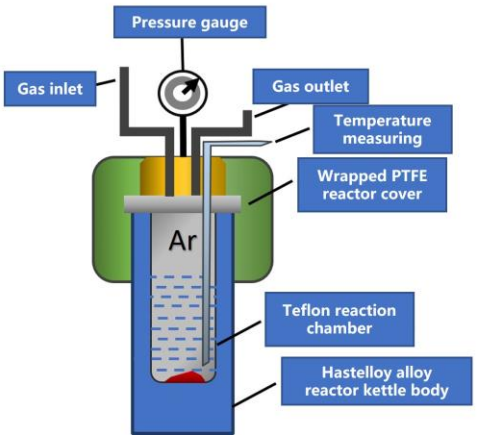

Fig. 1. *The hydrothermal reactor used for this study.*

A customized hydrothermal reactor was used for this experiment (Fig. 1). The effective volume is 50 mL. The reactor is made of Hastelloy. All the linings that might be in contact with the reactants are Teflon-coated to prevent any potential contamination of the serpentinization system from the reactor. A magnetic stirrer was equipped to stir throughout the experiments continuously. The head part is equipped with a temperature monitor, pressure gauge, air inlet and outlet devices. The air inlet and outlet are used to maintain the desired atmospheric conditions inside the reactor and collect gaseous products formed inside the reactor.

The initial and final composition of the solution samples, including the D/H ratios, were monitored for each experiment. The initial olivine and final solid products were analyzed by XRD, SEM-EDX, infrared spectroscopy, Mössbauer spectroscopy, and magnetic properties. Compositional and isotopic analyses of the

produced gas phases were also tried, but the concentrations were too low to detect.

Preliminary results: The solution of the Fa100 experiment shows a slight increase in pH (Table 1). In contrast, the other three Fe-bearing olivine samples (Fa71, Fa50, Fa29) all show a decrease in pH. The greater the initial Mg content was, the greater the reduction in pH.

Table 1. pH and D/H ratios of the experiments.

	Initial D/H	Final D/H	Initial pH	Final pH
Fa0	0.88	1.04	8.57	--
Fa29	0.93	1.00	9.29	8.04
Fa50	0.90	0.90	9.51	9.19
Fa71	0.93	1.03	8.67	8.45
Fa100	0.90	0.85	8.60	9.00

Note. The final pH of Fa0 was temporarily unavailable.

In addition, a comparison of the initial and final D/H ratios of the solution shows that, in general, the D/H ratios are increased except for Fa50 and Fa100. The Fa50 shows no changes in the D/H ratios, and the Fa100 experiment shows a slight decrease in the D/H ratios. Theoretically, D preferentially partitions into solid phases in the system, while H remains in the liquid phase. Further characteristics of solid alteration products and gaseous phases would be required to explain the D/H changes in the experiments.

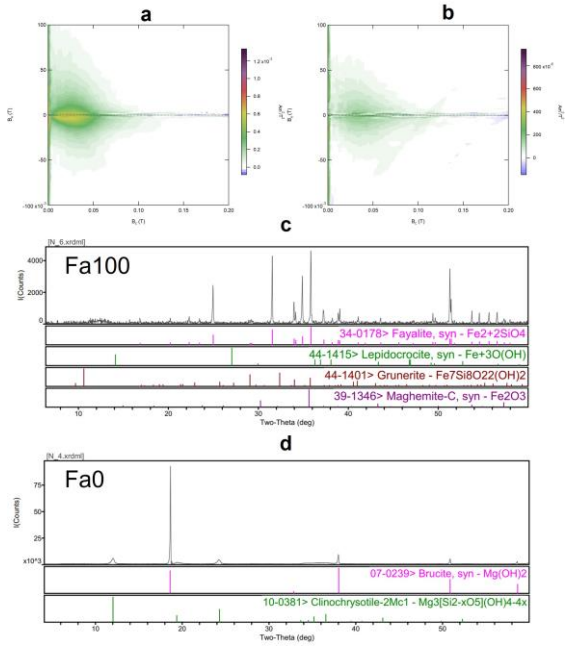

Figure 2: *(a) and (b) show the magnetic properties of the Fa100 samples before and after the experiment. (c) and (d) are the XRD patterns of the final products of Fa100 and Fa0, respectively.*

In the Fa100 experiment, magnetic analyses show that the magnetism properties weaken in the final products compared to the initial olivine (Fig. 2a, b). Previous studies suggested that when serpentinization reactions occur at $T \leq 200$°C, it is more likely to form serpentine and ferrite rather than magnetite [12, 13, 14]. This is one possible explanation of the observed disappearing magnetism in the final products. Consistently, the Mössbauer spectra also detected a new ferric species in the final products of Fa100, which is not magnetite.

In the Fa0 experiment, XRD patterns show that the final products are dominated by brucite (Fig. 2D) and that the reaction was close to completed.

Of all five olivines, secondary minerals are identified only in the Fa100 and Fa0 experiments. Considering that Fo almost completely transforms to brucite, it is generally speculated that reactions involving Mg-olivine should proceed further than those involving Fe-olivine. However, we find that reactions involving pure forsterite and fayalite can react faster than the Mg-Fe solid solution phases. Clinochrysotile was found in the Fa0 experiment, indicating that the reaction process reached the stage of serpentine production. The solution samples of the Fa100 experiment contain much less Si(aq) than those of the Fa50 experiment, presumably to form Fe-serpentine from Fe-brucite with Si(aq) (eq (1)). The newly formed ferric iron species in the final products of the Fa100 experiment may also indicate that Fe-serpentine is in the formation.

Data analysis is ongoing, and we will report completed results at the conference.

$$3(Mg,Fe)(OH)_2(Brucite)+2SiO_2(aq)=(Mg,Fe)_3Si_2O_5(OH)_4(serpentine)+H_2O \quad (1)$$

References: [1] Amador. E. S. et al. (2018) *Icarus, 311,* 113-114. [2] Etiope, G. and Sherwood Lollar, B. (2013) *ROG. Volume51, Issue2,* 276-299. [3] Hoefen. T. M. et al. (2003)*Science, 302 (5645).* 627-630, [4] Lin. H. L. et al. *(2021). Icarus, 355,* 114168. [5] McCollom. T. M. et al. (2016) *GCA, 181,* 175–200 [6] Koeppen. W. C. and Hamilton. V. E. (2008) *JGR-Planets, 113,* E5. [7] McCollom. T. M. et al. (2016) *GCA, 282,* 55-75 [8] Asaduzzaman. A. and Ganguly. J. (2021) *ACS Earth Space Chem. 5,* 880–889 [9] Escario. S. et al. (2018) *Lithos, 323,* 191-207. [10] Huang, R. et al. (2015) *Sci. China Earth Sci. 58,* 2165–2174. [11] Qi. C. et al. (2021) *JGR-Solid Earth, 126,* (3). [12] Klein. F. et al. (2013) *Lithos, 99,* 377–386; [13] Klein F. et al. (2014) *Geology, 42,* 135–138. [14] Seyfried, Jr., W. E. et al. (2007) *GCA, 71,* 3872–3886.